Adsorption Behaviors of Acidic and Basic Dyes by Thiourea-modified Nanocomposite Aerogels Based on Nanofibrillated Cellulose

Kai Liu,[a,*] Lihui Chen,[a] Liulian Huang,[a] Shan Lin,[a] Shilin Cao,[a] and Hongping Wang [b]

Inspired by the high adsorption efficiency of aerogels, a thiourea-modified nanocomposite aerogel consisting of nanofibrillated cellulose and chitosan was prepared *via* a facile method. The prepared novel aerogel was studied by Fourier transform infrared spectroscopy (FTIR) and scanning electron microscopy (SEM). The adsorptions of the acidic and basic dyes (acid orange 7 and crystal violet) on the aerogel from aqueous solutions were investigated according to the adsorption kinetics and isotherms. The results indicated that a pseudo-second-order kinetic model more accurately described the adsorption process than a pseudo-first-order model, and the adsorption processes of both acid orange 7 and crystal violet on the aerogel were controlled by both inter-facial and intra-particle diffusions simultaneously. The Langmuir isotherm was a better model as compared to Freundlich model for the adsorption of dyes. The aerogel prepared by the facile approach is a promising material for practical applications in acidic and basic dye removal.

Keywords: Nanofibrillated cellulose; Nanocomposite; Aerogel; Adsorption; Dye

*Contact information: a: College of Material Engineering, Fujian Agriculture and Forestry University, Fuzhou 350002, China; b: Jinshan College, Fujian Agriculture and Forestry University, Fuzhou 350002, China; *Corresponding author: E-mail: liuk1103@163.com*

INTRODUCTION

Water pollution induced by various dyes from industrial effluents is one of the most significant environmental problems; most dyes are non-degradable in the environment and are harmful to human health (Zhang *et al.* 2016; Bai *et al*. 2017). Consequently, there is an urgent need to decrease or remove the amount of dyes in industrial effluents. Many recent studies have focused on the application of various adsorbents for dye removal from aqueous solutions due to the relatively simple treatment process (Li *et al*. 2018). Among the adsorbents used, aerogel is one of the most effective adsorbent materials due to its high porosity, low density, and large surface area (Yang and Cranston 2014; Chong *et al.* 2015; Jiang *et al*. 2017; Martins *et al*. 2017). For example, Yang and Cranston (2014) prepared chemically cross-linked cellulose nanocrystal (CNC) aerogels based on hydrazine-crosslinking of hydrazide and aldehyde-functionalized CNCs; these CNC aerogels can absorb significant amounts of both water and dodecane.

Although various materials can be used to prepare aerogels, nanofibrillated cellulose and chitosan are two of the most widely used materials because of their biodegradability and high efficiency (Peng *et al.* 2014; Zhou *et al.* 2014; Zhang *et al.*

2015; Xu *et al.* 2016). Nanofibrillated cellulose (NFC) is a new form of expanded high-volume cellulosic material that is moderately degraded and greatly expanded in surface area. It is prepared through a homogenization process (Tanaka *et al.* 2016; Hubbe *et al.* 2017; Puangsin *et al.* 2017). NFC is a promising adsorbent material because of its large specific surface area and reactive surface hydroxyl groups. For example, Pei *et al.* (2013) prepared surface quaternized cellulose nanofibrils (Q-NFC) through a reaction of NFC and glycidyltrimethylammonium chloride. The resulting Q-NFC with trimethylammonium chloride contents of 0.59 to 2.31 mmol/g possessed high anionic dye adsorption capability. Moreover, the NFC possesses a network structure, leading to the rapid and effective removal of dyes from aqueous solution.

Chitosan (CS) is the second most abundant natural biopolymer after cellulose, and it is a promising adsorbent material due to the presence of abundant amino and hydroxyl groups that exhibit excellent chelating effects for various dyes (Zhu *et al.* 2012; Zhou *et al.* 2014). Zhou *et al.* (2011) prepared ethylenediamine-modified magnetic chitosan nanoparticles and demonstrated that the chitosan nanoparticles can be used for the effective adsorption of acidic dyes from aqueous solution.

Combining two or more polymers has attracted much interest because the composites can exhibit multi-functional properties (Abou El-Reash *et al.* 2011; Hu *et al.* 2011; Zhou *et al.* 2014). Chitosan and cellulose nanowhiskers can form a biodegradable nanocomposite by layer-by-layer technique due to the good biocompatibility and hydrophilic property of chitosan (Mesquita *et al.* 2010). In this study, chitosan was coated onto nanofibrillated cellulose (NFC/CS) to form a composite adsorbent. Furthermore, the composite adsorbent was modified with thiourea to increase the content of amino groups and thus improve the adsorption capacity of the composite. Finally, the thiourea-modified nanocomposite aerogels (T-NAs) were obtained by the freeze-drying treatment for T-NFC/CS. This novel aerogel was used to remove the acidic and basic dyes (acid orange 7 and crystal violet) from aqueous solution, and the adsorption characteristics of these dyes were investigated by the adsorption kinetics and isotherms.

EXPERIMENTAL

Materials

Nanofibrillated cellulose (NFC) (1%, w/w) was purchased from Tianjin Haojia Cellulose Co., Ltd. (Tianjin, China). The NFC with a width of 5 to 20 nm and a length of a few μm was produced from the softwood pulp and oxidized by TEMPO-oxidation. Chitosan (degree of deacetylation - 95%), thiourea, epichlorohydrin, acid orange 7 (AO7), and crystal violet (CV) were procured from Aladdin Reagent Co., Ltd (Tianjin, China). All other chemicals used were of analytical grade and used without further purification.

Preparation of Thiourea-modified Nanocomposite Aerogels (T-NAs)

Approximately 2 g of chitosan (CS) powder was dissolved in 100 mL of 5% (v/v) acetic acid solution, and 40 g of 1% NFC suspension was then added to the above solution. The mixture was stirred for 30 min. The NFC/CS nanocomposites were obtained by centrifuging the above mixture for 5 min at 8000 rpm.

The NFC/CS nanocomposites were modified with thiourea using a reported method with some modification (Zhou *et al.* 2009). Epichlorohydrin (10 mL) was dissolved in 90 mL of acetone. The NFC/CS nanocomposites were then added to the above solution, and stirred. After reacting for 4 h at 40 °C, 16 g thiourea was added to the mixture. After 4 h of reaction at 60 °C, 1 M NaOH solution (100 mL) was added to the mixture. After 2 h at 60 °C, the mixture was centrifuged and washed with distilled water for three times. The T-NAs aerogels were collected after slow freeze-drying the mixture.

FTIR Analysis

The FTIR spectra of the NFC, NFC/CS, and T-NAs were measured using a Fourier transform infrared spectrometer (Thermo Scientific Nicolet iS50, Waltham, MA, USA) in the spectral region of 500 to 4000 cm^{-1}. Prior to the measurement, each sample was freeze-dried and then pressed to thin pellets after mixing with KBr powder.

SEM Analysis

The fracture surface morphology of the NFC, NFC/CS, and T-NAs was observed using a scanning electron micrograph (Nova Nano SEM 230, FEI, Hillsboro, OR, USA). Each sample was first freeze-dried and then fractured in liquid nitrogen. The fracture surface of each sample was coated with gold in an ion sputter coater, and the operating voltage of SEM was kept at 5 kV.

Effect of pH on the Adsorption of Dyes

The effect of pH on the adsorption of various dyes was carried out by placing 10 mg T-NAs in 20 mL of 0.143 mmol/L AO7 or 0.0245 mmol/L CV dye solutions at different pH values. After shaking the mixture for 2 h at 30 °C at 200 rpm, the supernatant liquid was collected, and the dye concentration in the supernatant was measured at the maximum wavelength (λ_{max} 484 nm for AO7 and 590 nm for CV) using a Cary 300 UV-vis spectrophotometer (Agilent, Santa Clara, CA, USA).

The adsorption capacity of dye was calculated using Eq. 1 (Repo *et al.* 2011; Liu *et al.* 2015b),

$$q_e = \frac{(C_i - C_e)V}{m} \quad (1)$$

where q_e indicates the amount of dye adsorbed at equilibrium (mmol/g); C_i and C_e denote the initial and equilibrium concentrations of dye (mmol/L), respectively; m represents the mass of the T-NAs (g); and V denotes the volume of solution (L).

Adsorption Kinetics

The kinetic experiments of dye absorptions were conducted by placing 100 mg T-NAs in 200 mL of 0.143 mmol/L AO7 solution or 0.0245 mmol/L CV solution at the optimum pH (pH 3 for AO7 and pH 6 for CV). The mixture was then shaken at 30 °C and 200 rpm, and several milliliters of the supernatant liquid were removed at different time intervals for the measurement of the dye concentration. Three kinetic models were used to study the kinetics of the adsorption process.

The pseudo-first-order kinetic equation is given by Eq. 2 (Lagergren 1898),

$$\frac{1}{q_t} = \frac{K_1}{q_e t} + \frac{1}{q_e} \quad (2)$$

where K_1 is the pseudo-first-order rate constant (min^{-1}), and q_t and q_e ($mmol.g^{-1}$) denote the amount of dye adsorbed at time t (min) and at equilibrium, respectively.

The pseudo-second-order kinetic equation as expressed in Eq. 3 (Ho and McKay 1999),

$$\frac{1}{q_t} = \frac{1}{K_2 q_e^2} + \frac{1}{q_e} t \quad (3)$$

where K_2 is the pseudo-second-order rate constant (mmol/g/min).

Finally, the intra-particle diffusion model as described in Eq. 4 (Basha *et al*. 2009),

$$q_t = K_p t^{1/2} + C \quad (4)$$

where K_p is the intra-particle diffusion rate constant ($mmol.g^{-1}. min^{-1/2}$) and C indicates the adsorption constant.

Adsorption Isotherms

The adsorption isotherm experiments were performed by mixing 10 mg T-NAs with 20 mL dye solution with various concentrations at an optimum pH (pH 3 for AO7 and pH 6 for CV).

The initial concentrations of dye solution varied from 0.114 to 0.314 mmol/L for AO7 and 0.0245 to 0.0588 mmol/L for CV, respectively. The mixture was then shaken at 200 rpm and 30, 40, and 50 °C, respectively. After adsorption for 2 h, the dye concentrations in the supernatants were measured. Three isotherm models were used to study the isotherms of the adsorption process.

The Freundlich isotherm equation is given by Eq. 5 (Freundlich 1906),

$$\ln q_e = b_F \ln C_e + \ln K_F \quad (5)$$

The Langmuir isotherm equation is described by Eq. 6 (Langumuir 1918),

$$\frac{C_e}{q_e} = \frac{C_e}{q_m} + \frac{1}{q_m K_L} \quad (6)$$

where C_e represents the equilibrium concentration of dye (mmol/L); q_e is the amount of dye adsorbed at equilibrium (mmol/g); b_F and K_F are the Freundlich constants; K_L denotes the Langmuir constant (L/mmol); and q_m indicates the Langmuir maximum adsorption capacity of the dye (mmol/g).

Desorption and Reuse of the T-NAs

For the desorption and reusability studies, the T-NAs were separated and collected by centrifugation after the adsorption of dyes, and then washed with distilled water. About 200 mL NH_4OH/NH_4Cl (pH 10.0) for AO7 desorption or 50% (v/v) aqueous methanol solution for CV desorption were prepared and mixed with the washed T-NAs.

After agitating for 2 h at 30 °C, the T-NAs were collected and washed again with distilled water. Finally, the T-NAs after desorption were reused to adsorb for AO7 and CV at the optimum pH and 30 °C for 2 h. The above adsorption-desorption cycle was repeated three times.

RESULTS AND DISCUSSION

Preparation and Characterization of the Thiourea-Modified Nanocomposite Aerogels (T-NAs)

A facile approach for the preparation of the thiourea-modified nanocomposite aerogels (T-NAs) was developed in this study. The synthesis scheme of thiourea-modified NFC/CS nanocomposites is shown in Fig. 1. Initially, the nanofibrillated cellulose (NFC) was coated with chitosan, resulting in the introduction of amino groups to the NFC surface. After cross-linking by epichlorohydrin, the NFC/CS nanocomposites were modified with thiourea to increase the content of amino groups for the nanocomposites. Finally, the nanocomposites were freeze-dried to obtain the T-NAs.

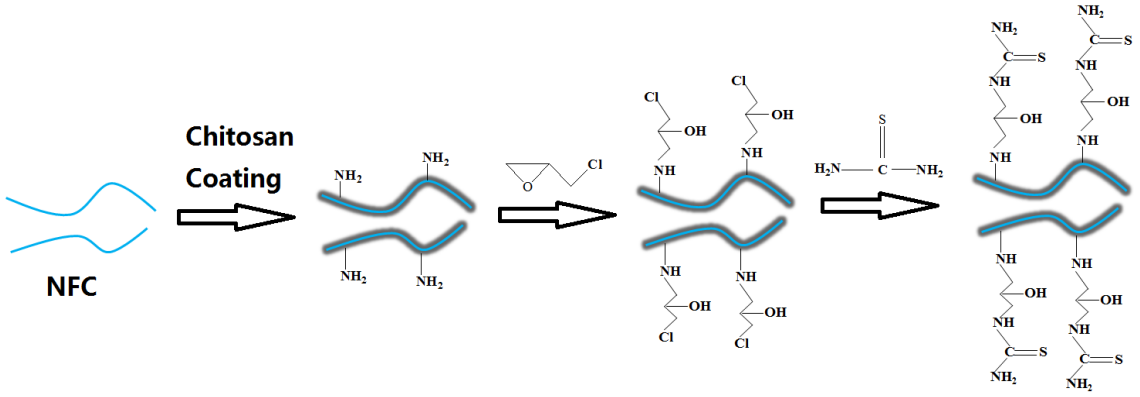

Fig. 1. Synthesis scheme of thiourea-modified NFC/CS nanocomposites

The FTIR spectra of NFC, NFC/CS, and T-NAs are shown in Fig. 2. The characteristic peaks at 3422, 2919, and 1456 cm^{-1} corresponded to O-H stretching, C-H stretching, and -CH_2 symmetric bending, respectively, which represented the typical bands of NFC (Liu *et al.* 2015a).

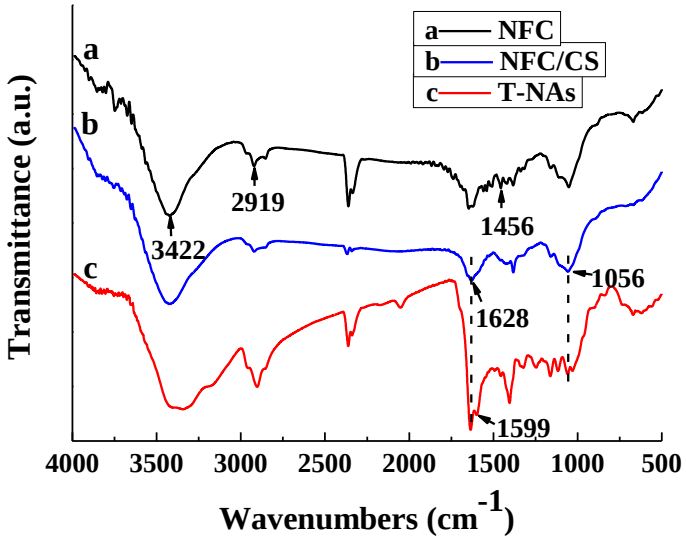

Fig. 2. The FTIR spectra of NFC, NFC/CS, and T-NAs

After coating with chitosan, several characteristic peaks of chitosan can be clearly observed. For instance, the peak at 1628 cm^{-1} was ascribed to the absorption of C=O group of chitosan (Cho *et al.* 2015), and the peak at 1056 cm^{-1} was assigned to the combined effects of C-N stretching vibration of primary amines and the C-O stretching vibration from the primary alcoholic group in chitosan (Zhou *et al.* 2009). After the modification of the NFC/CS with thiourea, several new characteristic peaks were introduced. For example, the peak found at 1599 cm^{-1} was attributed to C-N stretching of thiourea moiety (Zhou *et al.* 2009).

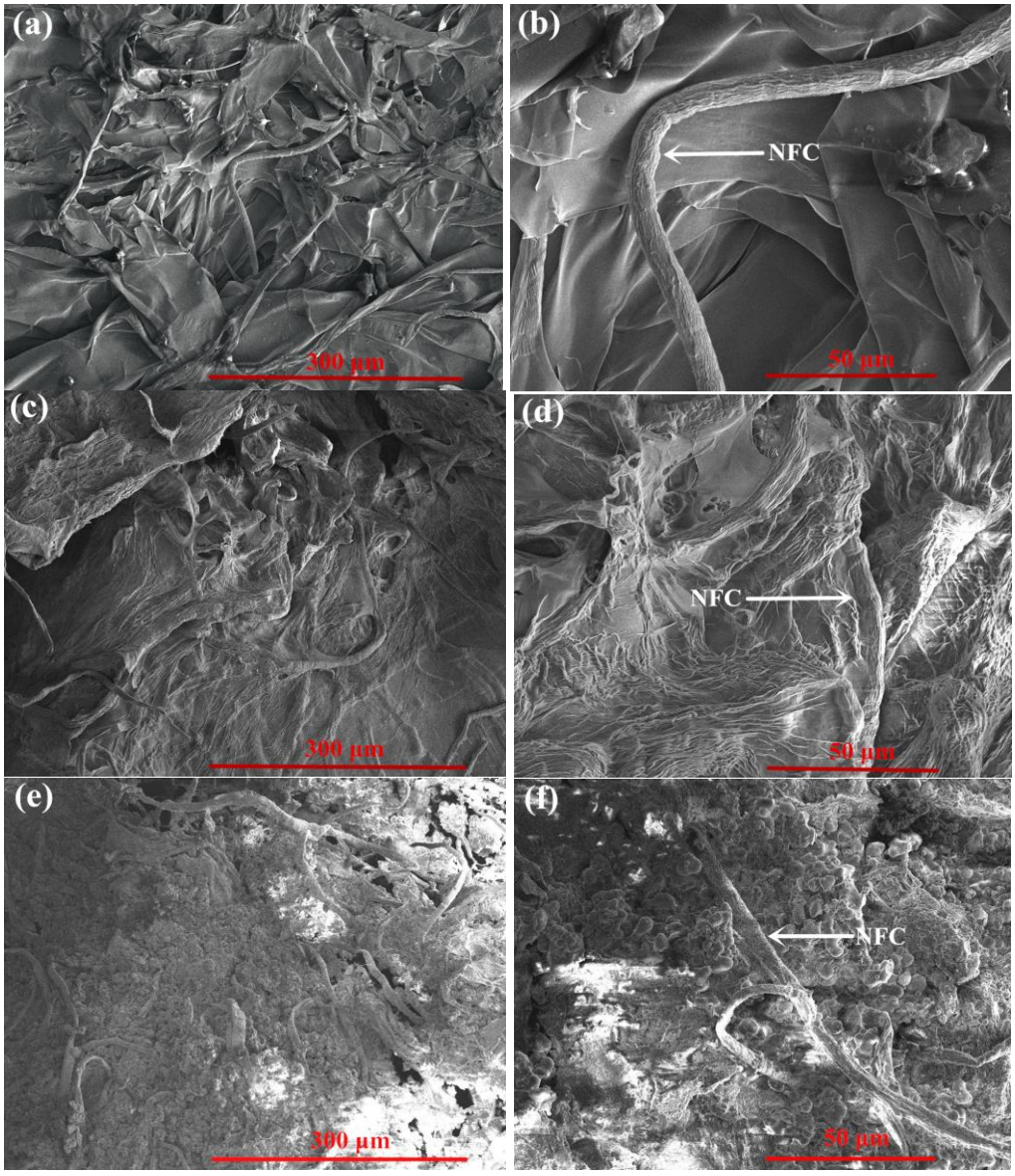

Fig. 3. SEM photographs of the cross-sections of (3a,b) NFC, (c,d) NFC/CS, and (e,f) T-NAs

Finally, the chitosan coating on the NFC and the modification of the NFC/CS nanocomposites with thiourea can be demonstrated by the SEM images of the cross-sections of the NFC, NFC/CA, and T-NAs, as shown in Fig. 3. As shown in Figs. 3a and

3b, several nanofibers with smooth surface cross-linked to form a network structure in the pure NFC aerogel. After chitosan coating on the NFC surface, a thin chitosan film can be observed to coat on the nanofiber surface (Figs. 3c and 3d). After the modification of the nanocomposites with thiourea, a lot of modified chitosan materials can be observed on the nanofibers (Figs. 3e and 3f). Moreover, the specific surface area of the aerogel (T-NAs) can reach 5.332 m^2/g and the pore diameter was about 3.410 nm.

Effect of pH

The solution pH plays a key role in the adsorption of dyes by aerogel absorbents. Therefore, the effect of pH on the adsorption of AO7 and CV on the T-NAs was studied, and the results are shown in Fig. 4. The initial pH of solution had substantial impact on the adsorptions of both acidic and basic dyes. The optimum pH was 3 and 6 for AO7 and CV, respectively. Similar results were found in previous studies. For example, Zhou *et al.* (2011) studied the effect of pH on the adsorption of AO7 on the modified magnetic chitosan nanoparticles. Yang *et al.* (2013) found that the best pH for CV absorption with the triphenylene-modified chitosan was about 7.

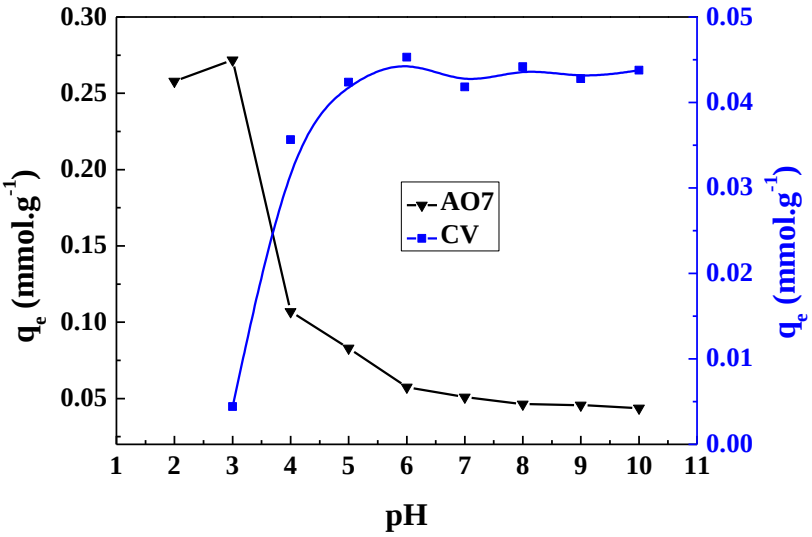

Fig. 4. Effect of solution pH on the adsorption of AO7 and CV on the T-NAs

Adsorption Kinetic Studies

The effect of time on the adsorptions of AO7 and CV dyes on the T-NAs is shown in Fig. 5a. The adsorption rates for both AO7 and CV were rapid, and the maximum adsorption was observed within 10 min for CV and 70 min for AO7, respectively. These rapid adsorptions of both acidic and basic dyes were due to the availability of plenty of active sites (amino groups) on the adsorbent surface after the modification of NFC/CS with thiourea. Similar results were found in previous research, where the adsorptions for both acid orange 7 (AO7) and acid orange 10 (AO10) on the modified magnetic chitosan nanoparticles were also rapid (Zhou *et al.* 2011).

To investigate the mechanism of adsorption, several typical kinetic models such as pseudo-first-order, pseudo-second-order, and intra-particle diffusion model were used,

and the results are shown in Fig. 5. The rate constants calculated using these models are listed in Table 1. Pseudo-second-order kinetics gave better agreement with the data for both AO7 and CV adsorptions. This is because of the higher coefficients of determination (R^2) of pseudo-second-order kinetics than those of pseudo-first-order kinetics. Several previous studies also reported that the adsorption of dyes on the chitosan were well described by the pseudo-second-order kinetic model (Yang *et al.* 2013; Cho *et al.* 2015).

Table 1. Pseudo-First-Order, Pseudo-Second-Order, and Intra-Particle Diffusion Constants, and their Correlation Coefficients

Dye	Pseudo-first-order			Pseudo-second-order		
	K_1(min^{-1})	q_e(mmol/g)	R^2	K_2(g.mmol^{-1}.min^{-1})	q_e(mmol/g)	R^2
AO7	2.287	0.222	0.9599	0.508	0.264	0.9969
CV	1.145	0.0436	0.9911	11.141	0.0451	0.9999
	Intra-particle diffusion					
	K_{p1}(mmol.g^{-1}. min$^{-1/2}$)		K_{p2}(mmol.g^{-1}. min$^{-1/2}$)	R_1^2	R_2^2	
AO7	0.0396		0.0113	0.9526	0.9427	
CV	0.00802		0.000712	0.9067	0.7966	

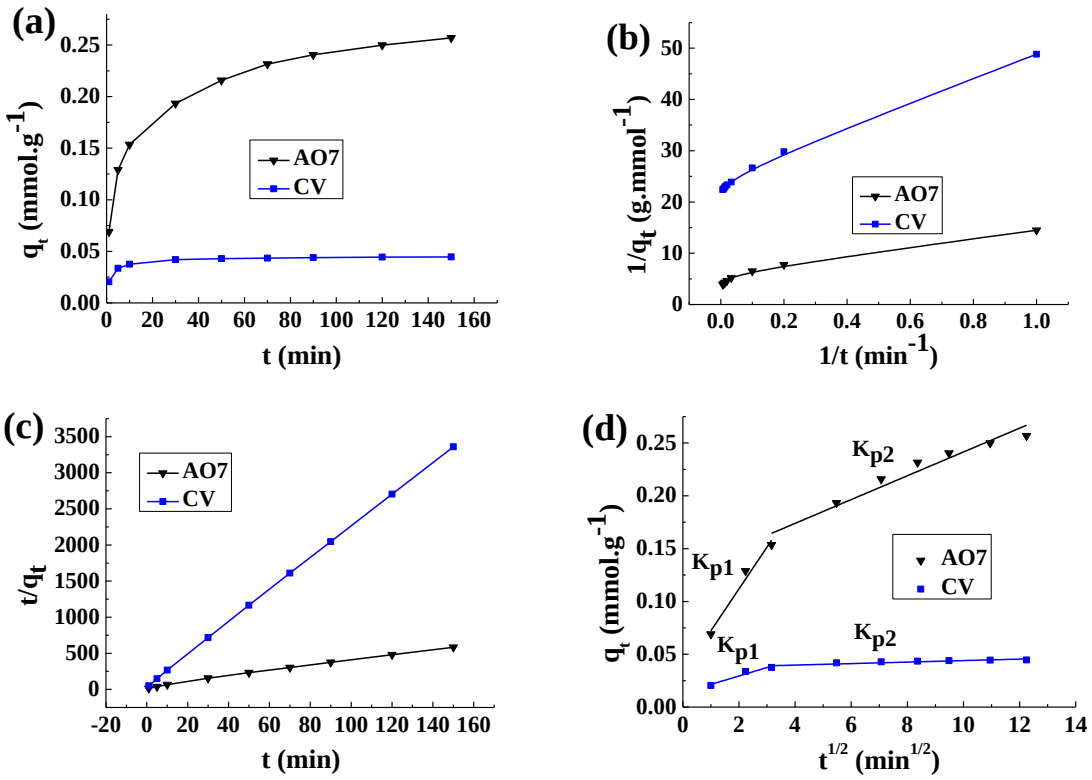

Fig. 5. Adsorption kinetics of AO7 and CV dyes by TNAs: (a) effect of time on the adsorptions of AO7 and CV on the T-NAs, (b) Pseudo-first order sorption kinetics, (c) Pseudo-second order sorption kinetics, and (d) Intra-particle diffusion kinetics.

In addition, the intra-particle diffusion model was applied to predict the rate-controlling steps. The adsorption process was controlled solely by intra-particle diffusion if the plot of q_t *versus* $t^{1/2}$ exhibited a single straight line. Otherwise it was controlled by

both interfacial and intra-particle diffusion if there were two distinctive lines in the plot of q_t *versus* $t^{1/2}$ (Cho *et al.* 2015). Figure 5d shows that the plot of q_t *versus* $t^{1/2}$ for both AO7 and CV adsorptions exhibited two straight lines, which indicated that the adsorption processes of these dyes on T-NAs were controlled by both interfacial and intra-particle diffusion simultaneously. Furthermore, the data in Table 1 show that the K_{p1} was much greater than the K_{p2} for both AO7 and CV, showing that the dyes were adsorbed on external binding sites on the adsorbent in the first phase, and then entered it into the pores of the adsorbent in the second phase after the external active sites were completely occupied by the dyes. Similar adsorption kinetic process of dyes on the magnetic chitosan composite can be found in a previous study (Cho *et al.* 2015).

Adsorption Isotherm Studies

For the adsorption isotherm studies, Langmuir and Freundlich equations were used, as shown in Figs. 6 and 7.

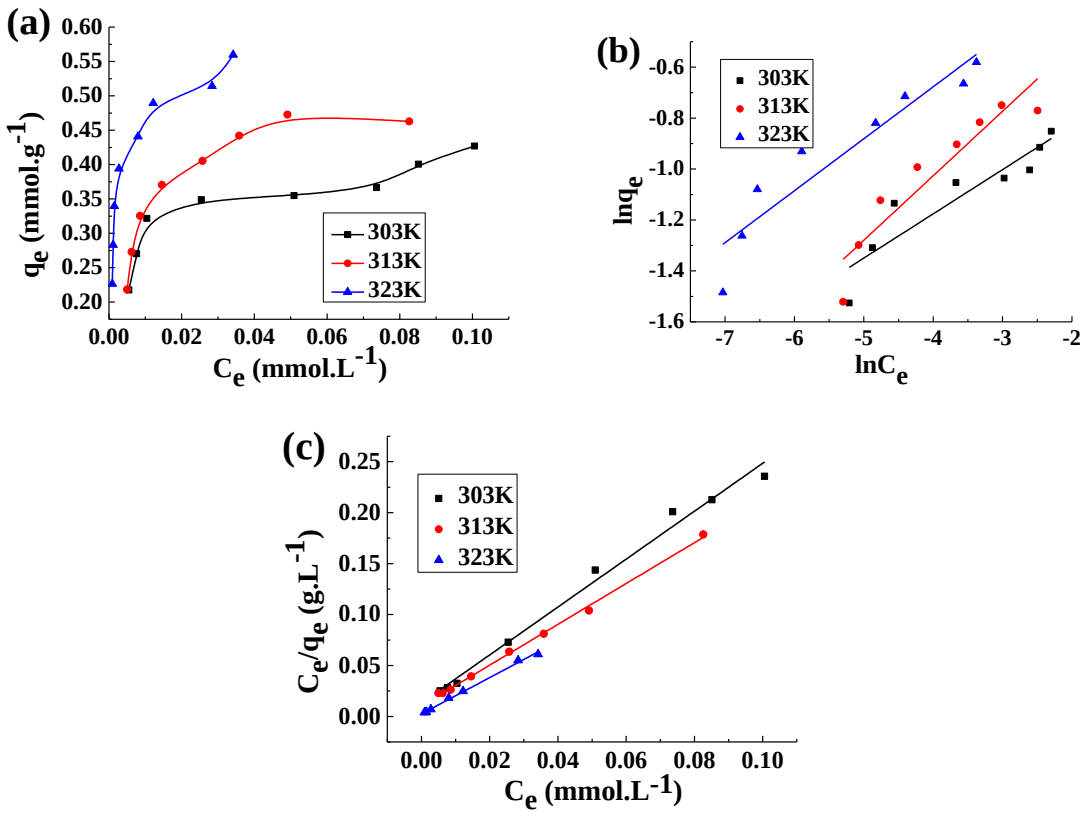

Fig. 6. Adsorption isotherms of AO7 by T-NAs: (a) effect of temperature on the adsorption of AO7, (b) Freundlich isotherm equation, and (c) Langmuir isotherm equation

The isotherm parameters were calculated from these models and are listed in Table 2. The coefficient of determination (R^2) of the Langmuir model for AO7 was higher than that of the Freundlich model under all the temperatures studied, indicating that Langmuir isotherm fitted better than Freundlich isotherm for AO7. For the adsorption isotherm of CV, the Langmuir isotherm was a better model than the Freundlich isotherm

due to the higher coefficients of determination at 40 and 50 °C. These results demonstrated that the adsorptions of AO7 and CV on the T-NAs' surface behaved as a monolayer sorption with independently acting sites of adsorption. Similar adsorption isotherm process for acidic and basic dyes on magnetic Fe/Ni nanoparticles was found in a previous study (Liu *et al.* 2015b).

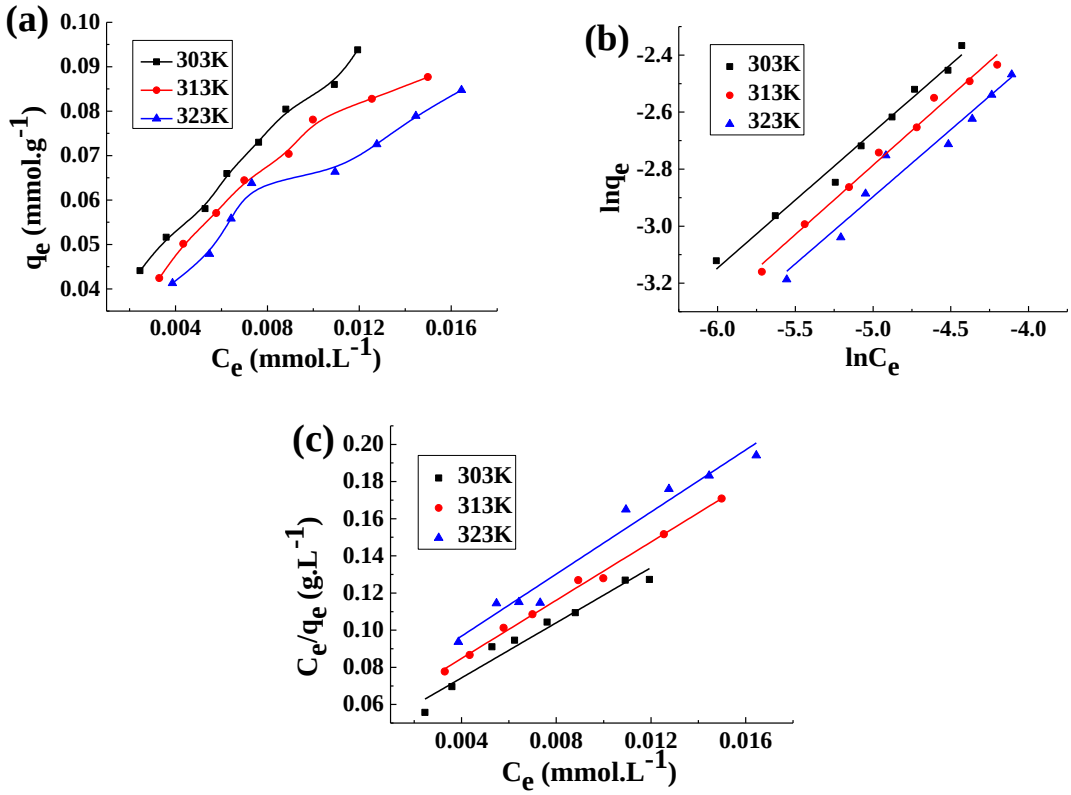

Fig. 7. Adsorption isotherms of CV by T-NAs: (a) effect of temperature on the adsorption of CV, (b) Freundlich isotherm equation, and (c) Langmuir isotherm equation

Table 2. Freundlich and Langmuir Isotherm Constants and their Correlation Coefficients

Dye	T(K)	Freundlich			Langmuir		
		K_F(mmol.g^{-1})	b_F	R^2	q_m(mmol.g^{-1})	K_L(L.mmol^{-1})	R^2
AO7	303	0.618	0.174	0.8498	0.425	175.418	0.9901
	313	0.986	0.253	0.8778	0.499	194.456	0.9979
	323	0.87	0.204	0.889	0.562	711.76	0.9965
CV	303	0.748	0.476	0.9866	0.135	165.919	0.963
	313	0.7	0.486	0.9894	0.128	146.736	0.9949
	323	0.581	0.471	0.9581	0.12	131.763	0.9702

It should be noted that the Langmuir maximum adsorption capacity (q_m) of AO7 under all the temperatures studied was much greater than that of CV. This may be due to the different adsorption mechanism for the acidic and basic dyes by the T-NAs. At the optimum pH (pH 3 for AO7), the amino groups of the T-NAs became protonated. The sulfonate groups of the acid dye (AO7) dissociate and were converted to dye anions,

resulting in the adsorption of AO7 on the T-NAs *via* ionic interaction (Zhou *et al.* 2011). However, the CV is cationic in solution; thus electrostatic attraction does not contributed to its adsorption on the T-NAs.

Desorption and Reusability Study

Desorption and reusabilities of T-NAs were tested using, NH_4OH/NH_4Cl and methanolic solutions were used as eluents for AO7 and CV desorptions, respectively. After desorption, the T-NAs were reused to adsorb dyes, and the results are shown in Fig. 8. The adsorption effectiveness of the T-NAs as adsorbent for AO7 and CV could still be maintained at about 66% and 22% levels after three repeated cycles, respectively. The variations in the regeneration characters for AO7 and CV may be ascribed to the different adsorption mechanisms for the acidic and basic dyes. Moreover, the decrease in the recyclability of the T-NAs for the dyes may be due to the shedding of the modified chitosan from the NFC during the desorption studies.

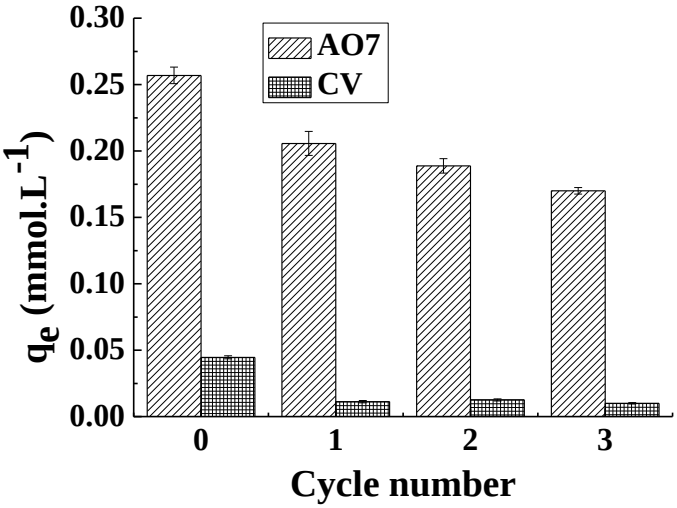

Fig. 8. Desorption and reusability of T-NAs

CONCLUSIONS

1. This research developed a facile method to prepare amino-rich aerogels for removing the acidic and basic dyes (AO7 and CV) from aqueous solutions.
2. According to the kinetic studies, pseudo-second-order kinetic model fitted better than pseudo-first-order for both AO7 and CV. The intra-particle diffusion model suggested that the adsorption processes of both AO7 and CV on the T-NAs were controlled by both interfacial and intra-particle diffusion simultaneously.
3. The adsorption isotherm studies indicated that the Langmuir maximum adsorption capacity (q_m) of AO7 under all the temperatures studied was much greater than that of CV due to the different adsorption mechanisms for the acidic and basic dyes by the T-NAs. Therefore, this new aerogel with excellent adsorption property may be used in dye wastewater treatment.

ACKNOWLEDGEMENTS

The authors are grateful to the special fund for science and technology innovation of Fujian Agriculture and Forestry University (KFA17551A, KFA17552A).

REFERENCES CITED

Abou El-Reash, Y. G., Otto, M., Kenawy, I. M., and Ouf, A. M. (2011). "Adsorption of Cr(VI) and As(V) ions by modified magnetic chitosan chelating resin," *Int. J. Biol. Macromol.* 49(4), 513-522. DOI: 10.1016/j.ijbiomac.2011.06.001

Bai, Q., Xiong, Q., Li, C., Shen, Y., and Uyama, H. (2017). "Hierarchical porous cellulose/activated carbon composite monolith for efficient adsorption of dyes," *Cellulose* 24(10), 4275-4289. DOI: 10.1007/s10570-017-1410-y

Basha, S., Murthy, Z.V.P., and Jha, B. (2009). "Sorption of Hg (II) onto Carica papaya: experimental studies and design of batch sorber," *Chem. Eng. J.* 147, 226-234. DOI: org/10.1016/j.cej.2008.07.005

Cho, D. -W., Jeon, B. -H., Chon, C. -M., Schwartz, F. W., Jeong, Y., and Song, H. (2015). "Magnetic chitosan composite for adsorption of cationic and anionic dyes in aqueous solution," *J. Ind. Eng.Chem.* 28, 60-66. DOI: 10.1016/j.jiec.2015.01.023

Chong, K. Y., Chia, C. H., Zakaria, S., Sajab, M. S., Chook, S. W., and Khiew, P. S. (2015). "$CaCO_3$-decorated cellulose aerogel for removal of Congo Red from aqueous solution," *Cellulose* 22(4), 2683-2691. DOI: 10.1007/s10570-015-0675-2

Freundlich, H.M.F. (1906). "Over the adsorption in solution," *J. Phys. Chem.* 57, 385-470.

Ho, Y. S., and McKay, G. (1999). "Pseudo-second order model for sorption processes," *Process Biochem.* 34, 451-465. DOI: 10.1016/S0032-9592(98)00112-5

Hubbe, M.A., Tayeb, P., Joyce, M., Tyagi, P., Kehoe, M., Dimic-Misic, K., and Pal, L. (2017). "Rheology of nanocellulose-rich aqueous suspensions: A review," *BioResources* 12(4), 9556-9661. DOI: 10.15376/biores.12.4.9556-9661

Hu, X. J., Wang, J. S., Liu, Y. G., Li, X., Zeng, G. M., Bao, Z. L., Zeng, X. X., Chen, A. W., and Long, F. (2011). "Adsorption of chromium (VI) by ethylenediamine-modified cross-linked magnetic chitosan resin: Isotherms, kinetics and thermodynamics," *J. Hazard. Mat.* 185(1), 306-314. DOI: 10.1016/j.jhazmat.2010.09.034

Jiang, F., Dinh, D. M., and Hsieh, Y. L. (2017). "Adsorption and desorption of cationic malachite green dye on cellulose nanofibril aerogels," *Carbohyd. Polym.* 173, 286-294. DOI: 10.1016/j.carbpol.2017.05.097

Lagergren, S. (1898). "Zur Theorie der sogenannten Adsorption geloster Stoffe," *Kungliga Svenska Vetenskapsakademiens* 24, 1-39.

Langmuir I. (1918). "The adsorption of gases on plane surfaces of glass, mica and platinum," *J. Am. Chem. Soc.* 40, 1361-1403.

Li, C., Lou, T., Yan, X., Long, Y. Z., Cui, G., and Wang, X. (2018). "Fabrication of pure chitosan nanofibrous membranes as effective absorbent for dye removal," *Int. J. Biol. Macromole.* 106, 768-774. DOI: 10.1016/j.ijbiomac.2017.08.072

Liu, K., Chen, L., Huang, L., Ni, Y., and Sun, B. (2015a). "Enhancing antibacterium and

strength of cellulosic paper by coating triclosan-loaded nanofibrillated cellulose (NFC)," *Carbohyd. Polym.* 117, 996-1001. DOI: 10.1016/j.carbpol.2014.10.014

Liu, Y., Zeng, G., Tang, L., Cai, Y., Pang, Y., Zhang, Y., Yang, G., Zhou, Y., He, X., and He, Y. (2015b). "Highly effective adsorption of cationic and anionic dyes on magnetic Fe/Ni (nanoparticles doped bimodal mesoporous carbon," *J. Colloid Interf. Sci.* 448, 451-459. DOI: 10.1016/j.jcis.2015.02.037

Martins, B. F., de Toledo, P. V., and Petri, D. F. (2017). "Hydroxypropyl methylcellulose based aerogels: Synthesis, characterization and application as adsorbents for wastewater pollutants," *Carbohyd. Polym.* 155, 173-181. DOI: 10.1016/j.carbpol.2016.08.082

Mesquita, J. O. P. d., Donnici, C. L., and Pereira, F. V. (2010). "Biobased nanocomposites from layer-by-layer assembly of cellulose nanowhiskers with chitosan," *Biomacromolecules* 11, 473-480. DOI: 10.1021/bm9011985

Pei, A., Butchosa, N., Berglund, L. A., and Zhou, Q. (2013). "Surface quaternized cellulose nanofibrils with high water absorbency and adsorption capacity for anionic dyes," *Soft Matter* 9, 2047-2055. DOI: 10.1039/c2sm27344f

Peng, S., Meng, H., Ouyang, Y., and Chang, J. (2014). "Nanoporous magnetic cellulose–chitosan composite microspheres: Preparation, characterization, and application for Cu(II) adsorption," *Ind. Eng. Chem. Res.* 53, 2106-2113. DOI: 10.1021/ie402855t

Puangsin, B., Soeta, H., Saito, T., and Isogai, A. (2017). "Characterization of cellulose nanofibrils prepared by direct TEMPO-mediated oxidation of hemp bast," *Cellulose* 24, 3767-3775. DOI: 10.1007/s10570-017-1390-y

Repo, E., Warchol, J. K., Bhatnagar, A., and Sillanpaa, M. (2011). "Heavy metals adsorption by novel EDTA-modified chitosan-silica hybrid materials," *J. Colloid Interf. Sci.* 358, 261-267. DOI: 10.1016/j.jcis.2011.02.059

Tanaka, R., Saito, T., Hanninen, T., Ono, Y., Hakalahti, M., Tammelin, T., and Isogai, A. (2016). "Viscoelastic properties of core-shell-structured, hemicellulose-rich nanofibrillated cellulose in dispersion and wet-film states," *Biomacromolecules* 17, 2104-2111. DOI: 10.1021/acs.biomac.6b00316

Xu, M. M., Bao, W. Q., Xu, S. P., Wang, X. H., and Sun, R. C. (2016). "Porous cellulose aerogels with high mechanical performance and their absorption behaviors," *BioResources* 11(1), 8-20. DOI: 10.15376/biores.11.1.8-20

Yang, F., Bai, X., Xu, B., and Guo, H. (2013). "Triphenylene-modified chitosan: novel high efficient sorbent for cationic and anionic dyes," *Cellulose* 20, 895-906. DOI: 10.1007/s10570-012-9856-4

Yang, X., and Cranston, E. D. (2014). "Chemically cross-linked cellulose nanocrystal aerogels with shape recovery and superabsorbent properties," *Chem. Mater.* 26, 6016-6025. DOI: 10.1021/cm502873c

Zhang, H., Luan, Q., Tang, H., Huang, F., Zheng, M., Deng, Q., Xiang, X., Yang, C., Shi, J., Zheng, C., and Zhou, Q. (2016). "Removal of methyl orange from aqueous solutions by adsorption on cellulose hydrogel assisted with Fe_2O_3 nanoparticles," *Cellulose* 24, 903-914. DOI: 10.1007/s10570-016-1129-1

Zhang, F., Wu, W. B., Sharma, S., Tong, G. L., and Deng, Y. L. (2015). "Synthesis of cyclodextrin-functionalized cellulose nanofibril aerogel as a highly effective adsorbent for phenol pollutant removal," *BioResources* 10(4), 7555-7568. DOI: 10.15376/biores.10.4.7555-7568

Zhou, L., Jin, J., Liu, Z., Liang, X., and Shang, C. (2011). "Adsorption of acid dyes from aqueous solutions by the ethylenediamine-modified magnetic chitosan nanoparticles," *J. Hazard. Mater.* 185, 1045-1052. DOI: 10.1016/j.jhazmat.2010.10.012

Zhou, L., Liu, J., and Liu, Z. (2009). "Adsorption of platinum(IV) and palladium(II) from aqueous solution by thiourea-modified chitosan microspheres," *J. Hazard. Mater.* 172, 439-446. DOI: 10.1016/j.jhazmat.2009.07.030

Zhou, Y., Fu, S., Zhang, L., Zhan, H., and Levit, M.V. (2014). "Use of carboxylated cellulose nanofibrils-filled magnetic chitosan hydrogel beads as adsorbents for Pb(II)," *Carbohyd. Polym.* 101, 75-82. DOI: 10.1016/j.carbpol.2013.08.055

Zhu, Y., Hu, J., and Wang, J. (2012). "Competitive adsorption of Pb(II), Cu(II) and Zn(II) onto xanthate-modified magnetic chitosan," *J. Hazard. Mater.* 221-222, 155-161. DOI: 10.1016/j.jhazmat.2012.04.026

Article submitted: March 29, 2018; Peer review completed: June 5, 2018; Revised version received and accepted: June 7, 2018; Published: June 12, 2018.
DOI: 10.15376/biores.13.3.5836-5849